MASS BALANCE OF CAMPBELL GLACIER, EAST ANTARCTICA, DERIVED FROM COSMO-SKYMED INTERFEROMETRIC SAR IMAGES

Hyangsun Han and Hoonyol Lee

Department of Geophysics, Kangwon National University, Republic of Korea

ABSTRACT

We derived tide-corrected ice-flow velocity map ($\mathbf{v}$ -map) of Campbell Glacier Tongue (CGT) in East Antarctica from 14 COSMO-SkyMed one-day tandem interferometric SAR image pairs obtained in 2011. Ice-flow velocity was measured to increase from the upper part of Campbell Glacier (~20 cm day^{-1}) to the seaward edge of CGT (~67 cm day^{-1}). Ice thinning rate by flux of CGT was obtained by calculating ice flux divergence from the $\mathbf{v}$ -map and the ice thickness of 340±18 m estimated by the ICESat GLAS data. Basal melting of CGT was deduced from the ice thickening rate (−6.29±1.37 m a^{-1}), surface mass balance (0.24±0.02 m a^{-1}) and the ice flux divergence. Total amount of ice loss in CGT (330.9±72.0 Mt a^{-1}) is more affected by ice flux divergence (214.6±26.7 Mt a^{-1}) than basal melting (129.2±56.4 Mt a^{-1}).

Index Terms— Campbell Glacier Tongue, DInSAR, ice-flow velocity, ice flux divergence, basal melting

1. INTRODUCTION

Outlet glaciers flow out of an ice sheet and forms ice shelf or ice tongue at the termination of the glacier. The temporal change in the thickness of ice shelve and ice tongue is controlled by ice thinning from ice flux, defined as ice flux divergence (*FD*), along with basal melting (*BM*) and surface mass balance (*SMB*), which influences the mass budget of an ice sheet considerably [1]. *FD* of the ice shelves and ice tongues can spatially vary in complicated manner because it is significantly affected by even the slight change in ice-flow velocity. Therefore, it is required to measure *FD* of ice shelves and ice tongues with high-spatial resolution and with high accuracy.

Differential interferometric SAR (DInSAR) technique can provide ice-flow velocity with centimeter accuracy. However, ice shelves and ice tongues experience vertical deflection due to the ocean tide as well as the gravitational ice-flow in the horizontal direction. As a result, DInSAR signals over an ice shelf or an ice tongue contain displacement components of both the horizontal ice-flow and the vertical tidal deflection during the interferometric data acquisitions [2]. The signal from the vertical tidal deflection should be removed from the DInSAR signals to measure accurate ice-flow velocity.

The vertical tidal deflection of an ice shelf can be estimated by double-differential interferometric SAR (DDInSAR) technique that differentiates two DInSAR signals by assuming that the gravitational ice-flow is steady during the observations [2]. The ratio of the vertical tidal deflection over tide height, defined as the tide deflection ratio, can be determined by a linear regression of the DDInSAR-derived tidal deflections with tidal variation [3]. It enables the estimation of the spatial variation of the vertical tidal deflection of the ice shelf for any tide height condition and thus the extraction of accurate ice-flow velocity from DInSAR signals.

In this study, we measure accurate ice-flow velocity of Campbell Glacier Tongue (CGT) in East Antarctica by removing the vertical tidal deflection from DInSAR signals, to calculate accurate mass budget of the glacier tongue.

2. STUDY AREA AND DATA

Campbell Glacier (74° 25′ S, 164° 22′ E), originated from the end of Mesa Range in Victoria Land in East Antarctica, is a fast-flowing outlet glacier with a length of about 110 km. Campbell Glacier flows into the Terra Nova Bay in Ross Sea and forms CGT that is a seaward extension of the glacier (Fig. 1). CGT is composed of two ice streams: the main stream of 13.5 km long and 4.5 km wide, and the branch stream of 8.0 km long and 2.5 km wide, respectively.

We used 14 one-day DInSAR pairs over CGT obtained from January to November 2011 (Table 1) by COSMO-SkyMed satellites. Among them, two images obtained on 25 October and 10 November 2011 were used to estimate ice-flow direction by performing the offset tracking method. The Global Digital Elevation Model (GDEM) from the Advanced Spaceborne Thermal Emission and Reflection Radiometer (ASTER) was used to remove topographic phases from the COSMO-SkyMed interferograms.

The Ross Sea Height-based Tidal Inverse Model (Ross_Inv) was used to predict tide height at a center point on CGT beyond the hinge zone. The effect of load tide was corrected by using the TPXO6.2 Load Tide model. The inverse barometer effect (IBE) of the predicted tide height was corrected by using in situ the atmospheric pressure data

Table 1. COSMO-SkyMed one-day tandem DInSAR pairs used in this study.

Dates	Perp. Baseline (m)	Tidal variation (cm)
2011/01/26, 2011/01/27	18.9	-11.6
2011/02/27, 2011/02/28	5.7	-4.5
2011/03/15, 2011/03/16	-44.4	-17.5
2011/03/31, 2011/04/01	-39.2	8.3
2011/05/02, 2011/05/03	-89.6	8.3
2011/05/18, 2011/05/19	75.9	27.8
2011/06/03, 2011/06/04	-36.5	-3.3
2011/06/19, 2011/06/20	-47.5	-14.7
2011/08/22, 2011/08/23	181.7	27.6
2011/09/07, 2011/09/08	37.3	1.0
2011/10/09, 2011/10/10	-44.4	5.8
2011/10/25, 2011/10/26	-110.9	-14.0
2011/11/10, 2011/11/11	-91.7	2.0
2011/11/26, 2011/11/27	-23.4	7.5

measured by an automatic weather system installed near CGT. We also used the map of tide deflection ratio (α) of CGT, which was generated by performing linear regression analysis between the DDInSAR-derived tidal deflection and tidal variations predicted by the IBE-corrected Ross_Inv [3].

Surface elevation of CGT measured by the Geoscience Laser Altimetry System (GLAS) onboard the Ice, Cloud, and land Elevation Satellite (ICESat) was used to estimate ice thickness of the glacier tongue. We obtained 7 ICESat GLAS measurements of the same ground track across CGT from March 2005 to November 2008. We corrected tidal effect on the ICESat GLAS surface elevation data by using tide height predicted by the Ross_Inv. The IBE was corrected by using the surface level atmospheric pressure data from the ERA-Interim reanalysis. We used *SMB* over CGT simulated by the Regional Atmospheric Climate Model (RACMO) [4].

3. METHOD

First, we generate 14 one-day tandem differential interferograms by performing 2-pass DInSAR technique by removing topographic phase using the ASTER GDEM. DInSAR signals of an ice tongue (ϕ_{LOS}) represent surface displacement in the line of sight (LOS) direction, which is the summation of the horizontal ice-flow (ϕ_{LOS}^{flow}) and the vertical tidal deflection (ϕ_{LOS}^{tide}). To account for ϕ_{LOS}^{tide}, we use α, defined as the ratio of the vertical tidal deflection of ice over tide height (T). For one-day DInSAR signals, the difference of the vertical tidal deflection is related to one-day difference of T, defined here as $\dot{T}$. Therefore, ϕ_{LOS}^{tide} in one-day DInSAR signals can be represented as

$$\phi_{LOS}^{tide} = \alpha \dot{T} \cos\theta \qquad (1)$$

where θ is radar look angle. ϕ_{LOS}^{flow} of an ice tongue can be estimated by removing ϕ_{LOS}^{tide} from ϕ_{LOS}.

ϕ_{LOS}^{flow} represents an ice-flow component in the LOS direction, but not in actual flow direction. To determine ice-flow direction, we perform the offset tracking between the COSMO-SkyMed SAR images obtained on 25 October and 10 November 2011. By assuming that ice-flow direction is stable during a year in 2011, we convert the observed ice-flow in the LOS direction to that in the flow direction estimated from the offset tracking results. We then generate a map of averaged ice-flow velocity ($\mathbf{v}$ -map) and its standard deviation (σ_v -map) from the 14 DInSAR-derived one-day ice-flows to represent annual state of the glacier flow.

FD at any point on an ice tongue is defined as [1]

$$FD = \nabla \cdot (H\mathbf{v}) \qquad (2)$$

where H is the ice thickness and $\mathbf{v}$ is the ice-flow velocity obtained in the previous section. H can be estimated from the ice surface elevation (h) by assuming that ice is in a state of hydrostatic equilibrium. We use h beyond the hinge zone of CGT measured by the ICESat GLAS from 2005 to 2008, which is averaged to lower the random noises included in individual observations and to find a representative h value over the whole CGT for a long-term stage. The calculated FD is gridded to a 5 m spacing.

We estimate BM of CGT by using the mass conservation equation defined as [1]

$$\partial H/\partial t = SMB - FD - BM \qquad (3)$$

where $\partial H/\partial t$ is the ice thickening rate, SMB is surface mass balance, FD is ice flux divergence, and BM is bottom melting, respectively. A SMB value modeled by the RACMO was used for the whole CGT. A $\partial H/\partial t$ value for the whole CGT was estimated by using the h measured by the ICESat GLAS.

BM calculated by the equation (3) uses the FD that provides very accurate ice thinning rate with high-spatial resolution by correcting tidal effect included in the DInSAR signals of CGT including the hinge zone. This is a major improvement in the estimation of the BM in this study when compared with the previous studies that calculated from the DInSAR-derived ice flux divergence without adequate correction of tidal effect contained in the DInSAR signal especially in the hinge zone.

4. RESULT AND DISCUSSION

We removed signals of ϕ_{LOS}^{tide} from the DInSAR images and extracted ϕ_{LOS}^{flow} over CGT. By using the ice flow direction obtained from the offset tracking method and the ice speed rotated from the LOS ice speed, we generated the $\mathbf{v}$-map and σ_v-map as shown in Fig. 1(a) and 1(b), respectively.

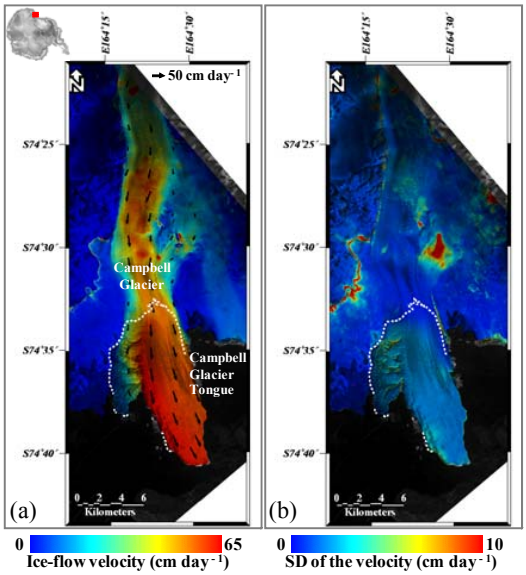

Fig. 1. (a) Average one-day ice-flow velocity in the ice-flow direction of Campbell Glacier and CGT and (b) its standard deviation (SD).

The white dotted lines in Fig. 1 represent the location of grounding line. The black arrows in Fig. 1(a) represent the ice-flow directions estimated by the offset tracking results. Ice-flow velocity gradually increases from the upper grounded part of Campbell Glacier (~20 cm day^{-1}) to the seaward edge of CGT (~67 cm day^{-1}), and from the glacial margins to the central flow line of the glacier.

Within the hinge zone of the main stream of CGT, ice-flow velocity increases along the flow line from grounding line (~52 cm day^{-1}) to the seaward edge of the hinge zone (~62 cm day^{-1}). However, ice-flow velocity of the free-floating zone is almost constant along the flow line. The eastern part of the main stream of CGT flows slower than the western part. This is related to the geometry of grounding line which is parallel to the flow direction [3]. Therefore, ice-flow slows down due to basal drag in the eastern part while that of the western part increases after the grounding line. The branch stream of CGT shows spatially irregular ice-flow due to the random motion of the broken ice chunks [3].

Most areas of the grounded part of Campbell Glacier show small σ_v less than ~2 cm day^{-1}, indicating that ice-flow velocity is steady with time. However, some regions show σ_v values larger than 10 cm day^{-1} due to the insensitivity of the DInSAR signal to the ice-flow in azimuth direction of SAR coordinates. The more ice-flow line is out of the LOS direction, the less the sensitivity of the DInSAR-measured ice-flow is. The ice flow direction of those regions is almost perpendicular to the LOS direction (Fig. 1).

σ_v values on the main stream of CGT are ~4 cm day^{-1}, which are twice the values on the grounded part of Campbell Glacier. This is caused by the uncertainty of the α-map, especially by the error of tide height predicted by Ross_Inv. However, the σ_v values of ~4 cm day^{-1} are equivalent to only ~6% of ice-flow velocity of CGT. Some regions of the branch stream of CGT show large σ_v values due to random motion of the broken ice chunk. Therefore, we will focus on the main stream of CGT only for further analysis.

We calculated ice thinning rate by flux (FD) of the main stream of CGT by using the $\mathbf{v}$-map and H of 340±18 m. Fig. 2(a) and 2(b) show FD (m a^{-1} in water equivalent) of the main stream of CGT and its uncertainty, respectively. The white solid lines represent the location of grounding line and a white dotted line represents the seaward edge of hinge zone of the main stream of CGT. FD varies spatially from −2 to 25 m a^{-1} with the uncertainty less than 2 m a^{-1}. Positive values, representing ice thinning by flux, are dominant over the glacier tongue with an average value of 4.08±0.51 m a^{-1} over the main stream of CGT.

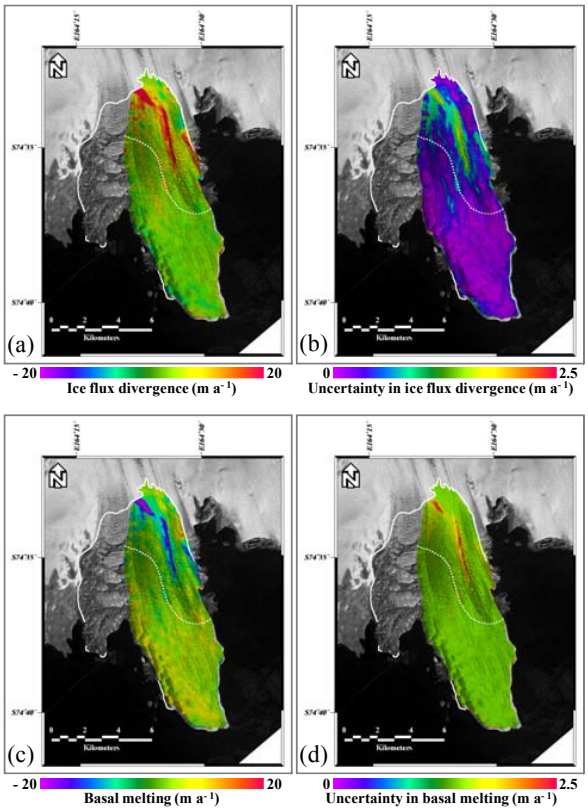

Fig. 2 (a) Ice flux divergence (in water equivalent) of the main stream of Campbell Glacier Tongue and (b) its uncertainty. (c) Basal melting (in water equivalent) deduced by employing the ice flux divergence and (d) its uncertainty.

FD are very large within the hinge zone due to rapidly increasing ice-flow velocity while that beyond the hinge zone (the free-floating zone) are close to zero because ice-flow velocity is almost constant. This represents that ice thinning by flux is more considerable within the hinge zone than the free-floating zone. The ice thinning rate is noticeably high along the ice-flow lines at the central-eastern part of the hinge zone (illustrated as red color in Fig. 2a), which results from the variation of the ice-flow velocity increasing from the eastern part to the western part of CGT due to the grounding line located along the eastern edge of the glacier tongue. This high ice thinning zone locates the boundary between the region of severe basal drag and the free-flowing region.

Using *FD* -map, *BM* of the main stream of CGT was calculated by assuming that *H* and *SMB* in equation (3) are constant over the CGT. *SMB* value of 0.24±0.02 m a^{-1} in water equivalent was calculated by averaging the monthly *SMB* fields around CGT for the period from January 1979 to July 2012 from the RACMO. $\partial H/\partial t$ of CGT was estimated to be −6.29±1.37 m a^{-1} (in water equivalent).

BM of the main stream of CGT and its uncertainty (m a^{-1} in water equivalent) are shown in Fig. 2(c) and 2(d), respectively. Most areas of the main stream of CGT show positive *BM* values which mean melting of ice bottom. *BM* values within the hinge zone are smaller than those beyond the hinge zone, of which the aspect of the spatial variation is opposed to that of *FD* (Fig. 2a). Negative values of *BM* are observed in some regions within the hinge zone where ice thins by large *FD* (illustrated as purple color in Fig. 2c), which represents that ice bottom is freezing to restore the mass loss by outward flux.

Bottom melting beyond the hinge zone of the main stream of CGT is very considerable, especially near the ice front by ~10±2 m a^{-1}. The spatial variation of *BM* over CGT suggests that the impact of warm deep water circulation, the cause of basal melting of an ice shelf [5], increases towards the ice front. Area-average *BM* of the main stream of CGT is 2.46±1.56 m a^{-1}.

The above rates can be converted to mass budget by multiplying the area (52.6 km^2) of the main stream of CGT. By assuming constant values of *SMB* and $\partial H/\partial t$ of 12.8±0.4 Mt a^{-1} (megatons per year) and −330.9±72.0 Mt a^{-1}, respectively, and using the total *FD* of 214.6±26.7 Mt a^{-1}, total *BM* of the main stream of CGT is calculated to be 129.2±56.4 Mt a^{-1} (water mass equivalent). This represents that ice thinning by flux and bottom melting of the main stream of CGT is progressing much faster than snow accumulation over the surface of the glacier tongue. Note that *FD* is about two times larger than total *BM* , from which we could confirm that ice flux divergence is the main cause of the ice thinning of the main stream of CGT than basal melting.

5. CONCLUSION

We measured ice-flow velocity over CGT by removing the vertical tidal deflection from the 14 COSMO-SkyMed one-day tandem DInSAR images. Ice-flow velocity increased from the upper part of Campbell Glacier to the seaward edge of CGT and it was steady with time. However, the branch stream of CGT shows random motion by the broken ice chunks. Ice-flow velocity within the hinge zone of the main stream of CGT increases from grounding line to the seaward edge of the hinge zone, while that beyond the hinge zone is almost constant along the flow line.

Ice flux divergence with high spatial resolution over the main stream of CGT was derived from the ice-flow velocity. Ice thinning by flux within the hinge zone of CGT is more considerable than that beyond the hinge zone. Basal melting of CGT was derived by employing the ice flux divergence. The main stream of CGT experiences bottom melting, except for some regions within the hinge zone where ice thins largely due to flux. Basal melting beyond the hinge zone, especially near the ice front, is very considerable compared to that within the hinge zone.

By comparing total ice flux divergence with total basal melting, we could confirm that temporal change in ice thickness of the main stream of CGT is more affected by the ice flux divergence than basal melting by 35%.

ACKNOWLEDGMENTS

This work was supported by Basic Science Research Program through the National Research Foundation of Korea (NRF) funded by the Ministry of Education (NRF-2013R1A1A2008062) and also by Space Core Technology Development Program through the NRF funded by the Ministry of Science, ICT and Future Planning (NRF-2013M1A3A3A02041853).

REFERENCES

[1] E. Rignot, S. Jacobs, J. Mouginot, and B. Scheuchl, "Ice-shelf melting around Antarctica," *Science*, 341(6143), pp. 266–270, 2013.

[2] E. Rignot, J. Mouginot, and B. Scheuchl, "Antarctic grounding line mapping from differential satellite radar interferometry," *Geophysical Research Letters*, 38, L10504, 2011.

[3] H. Han and H. Lee, "Tide deflection of Campbell Glacier Tongue, Antarctica, analyzed by double-differential SAR interferometry and finite element method," *Remote Sensing of Environment*, 141, pp. 201–213, 2014.

[4] J.T.M. Lenaerts, M.R. van den Broeke, W.J. van de Berg, E. van Meijgaard, and P. Kuipers Munneke, "A new, high-resolution surface mass balance map of Antarctica (1979–2010) based on regional atmospheric climate modeling," *Geophysical Research Letters*, 39, L04501, 2012.

[5] S. S. Jacobs, H. Hellmer, C.S.M. Doake, A. Jenkins, and R. Frolich, "Melting of ice shelves and the mass balance of Antarctica," *Journal of Glaciology*, 38(130), pp. 375–387, 1992.